



SOLID STATE ELECTRONICS LABORATORY

DEPARTMENT OF ELECTRICAL ENGINEERING
STANFORD UNIVERSITY • STANFORD, CA 94305
TELEPHONE: FAX: 415-723-4659

July 16, 1996

Defense Technical Information Center
Building 5, Cameron Station
Alexandria, Virginia 22304-6145

Dear Sir:

Please find enclosed one copy of the monthly progress reports for the months of March, April, May, and June 1996 for contract N00014-92-J-1996 entitled "Low Voltage Electron Beam Lithography".

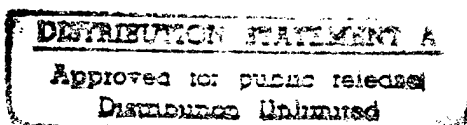
Sincerely,

R. Fabian Pease
Professor of Electrical
Engineering

se

Encls.

cc: Ruth Kaempf
Susan Skulina



DMC QUALITY INSPECTED 3



DEPARTMENT OF THE NAVY
OFFICE OF NAVAL RESEARCH
SEATTLE REGIONAL OFFICE
1107 NE 45TH STREET, SUITE 350
SEATTLE WA 98105-4631

IN REPLY REFER TO:

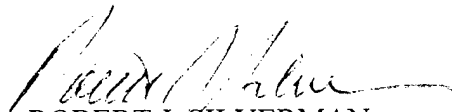
4330
ONR 247
11 Jul 97

From: Director, Office of Naval Research, Seattle Regional Office, 1107 NE 45th St., Suite 350,
Seattle, WA 98105
To: Defense Technical Center, Attn: P. Mawby, 8725 John J. Kingman Rd., Suite 0944,
Ft. Belvoir, VA 22060-6218

Subj: RETURNED GRANTEE/CONTRACTOR TECHNICAL REPORTS

1. This confirms our conversations of 27 Feb 97 and 11 Jul 97. Enclosed are a number of technical reports which were returned to our agency for lack of clear distribution availability statement. This confirms that all reports are unclassified and are "APPROVED FOR PUBLIC RELEASE" with no restrictions.

2. Please contact me if you require additional information. My e-mail is *silverr@onr.navy.mil* and my phone is (206) 625-3196.


ROBERT J. SILVERMAN

ARPA Monthly Progress Reports for James Schneider

March and April:

In April, processing of NEA cathodes for activation commenced. The final preparations of the UHV chamber for the processing were made, and the wet processing sequence for the cathodes was set up. Additional work was done on completing the Monte Carlo simulator for investigating the statistical Coulomb interactions for parallel electron beam direct write systems.

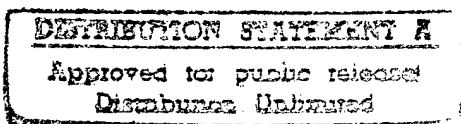
May:

First successful activation of cathodes to true negative electron affinity was achieved in a UHV system with 6 microamps of total current at 21% quantum efficiency, with no visible decay in cathode conditions over a 12 hour test period. These results are very encouraging for the forthcoming construction of the electron gun, which will begin next month.

The Monte Carlo simulator was completed. This versatile program allows for the investigation of space charge effects in parallel beam systems. The first test cases for this program were on a telecentric demagnifying system that might be used in a direct write electron beam lithography application. The results of these simulations were presented by me at the Electron, Ion, and Photon Beams and Nanofabrication Conference (Three Beams) in Atlanta on May 30, 1996. A preprint of this work is enclosed. Several cathode configurations were considered, and several encouraging results were found. First, for a cathode with a 0.5 micron source size, and a total of 0.5 microamps total emitted current, the beam blurring is less than 10 nm, which is acceptable for a 0.1 micron design rule. Moreover, the low energy spread of the negative electron affinity cathode allows for a very large amount of the total current (36% of the generated current) to be delivered to the wafer. For a patterned cathode surface with a 0.1 micron source size, a much smaller demagnification may be used, and hence all of the current generated at the source may be delivered to the wafer. Therefore, for a given throughput, a smaller amount of generated current is required, reducing the total beam blurring for a patterned cathode.

June:

Construction of the electron gun and processing of the electron optical components began. Moreover, a scheme was developed whereby the emitted current from the NEA cathode could be stabilized over a period of more than 48 hours.



19970716 148

DTIC QUALITY INSPECTED 3

ARPA Monthly Progress Reports for Aaron Baum

March and April 1996:

Successfully re-sealed and baked out cathode activation chamber, achieving good ultra-high vacuum conditions for a cathode activation. Prepared an Intevac-provided, modified photocathode for activation using Intevac methods. Transferred photocathode into system and attempted to activate using Cs and O₂. Small photoresponse seen. Continuing machining and final designing of electron gun parts.

May 1996:

Small photoresponse found to be due to charging caused by poor cathode contact. Removed cathode, remachined cathode holder, improved holder to emitting surface contacts. Reintroduced to system and activated cathode to 21% quantum efficiency with 633nm light, an efficiency comparable to the best commercial cathodes, many times better than that achieved by other researchers in the field. On a subsequent activation, eleven hours of stable emission are observed.

Continuing machining and final designing of electron gun parts. Initial assembly of electron gun.

June 1996:

Over 48 hours of stable emission from the photocathode are achieved, with a clear potential for longer times; the experiment was interrupted by a blown fuse in the signal-detecting lock-in, while the emission had not degraded at all over the whole period.

Most electron gun parts received, assembly continued.

Semiconductor on Glass Photocathodes as High-Performance Sources for Parallel Electron Beam Lithography

**J. E. Schneider, A. W. Baum, G. I. Winograd, R.F.W. Pease,
M. McCord and W.E. Spicer**
*Solid State Electronics Laboratory
Stanford University
Stanford, CA*

K. A. Costello and V. W. Aebi
*Intevac, Inc. Advanced Technologies Division
Santa Clara, CA*

ABSTRACT

The throughput of electron beam lithography has historically been limited by electron-electron interactions that cause blurring at high currents. We present a system configuration for maskless parallel electron beam lithography using a new multiple primary source technology that, by employing widely spaced beams, significantly reduces this problem. The proposed source technology, a negative electron affinity (NEA) photocathode, allows us to generate an array of high brightness, low energy spread, independently modulated beams over a large area. In order to assess the effects of electron-electron interactions in this system, Monte Carlo simulations have been performed. The results of these calculations indicate that this configuration enjoys significant advantages over existing maskless systems. By restricting the area of emission for the individual beamlets to submicron dimensions, the blurring due to statistical electron-electron interactions can be significantly reduced for a given current at the wafer. For example, at 50 kV a total current of more than 2.5 μA can be obtained with less than 10 nm beam blurring. Preliminary experimental results suggest that high brightness emission can be maintained from an NEA photocathode in a demountable vacuum system.

I. INTRODUCTION

One subject of intense research in recent years has been the possibility of increasing the throughput of electron beam direct write technology to be competitive for wafer production for linewidths of $0.1\text{ }\mu\text{m}$ and below. It has been recognized that the most straightforward way of achieving higher throughput direct write equipment is to dramatically increase the current in the electron beam column (without increasing the landing energy). Several prototype systems have been proposed which rely upon the generation of an extended, high-current (several microamps) exposing beam for electron or ion image projection¹⁻⁵. Other proposed systems have included the use of a large array of secondary sources or blanking apertures following a wide-area, collimated beam.^{6,7} It has been suggested, however, that by using multiple primary sources, useful throughput may be achieved for total currents at the wafer between 0.5 and a few microamps.⁸ Here we propose a new system configuration in which multiplexed primary sources illuminate the wafer through the use of a simple, two lens demagnifying projection system. Because the system employs an array of independently modulated Gaussian beams, a raster scan system can be used that has the advantage of being maskless. The centerpiece of this configuration is a new parallel electron source technology currently under development in our laboratory.

The proposed source, a negative electron affinity (NEA) photocathode, has thus far been used in high efficiency image intensifiers for night vision applications, as well as in specialty electron sources for experimental particle physics. Recently, however, Baum et al. demonstrated excellent source properties experimentally in specially modified night vision tubes.^{9,10} Beam brightnesses of $1 \times 10^8\text{ A}/(\text{cm}^2\text{ sr})$ from a $1.7\text{ }\mu\text{m}$ diameter illuminating spot, as well as energy spreads of 50-200 meV, have been measured. In addition to these properties, NEA photocathodes also exhibit highly uniform emission to within 5% over a large area (100 mm^2), and have picosecond-scale switching times.¹¹ Moreover, since these cathodes are fabricated from GaAs, they may be excited with visible red diode lasers at 635 nm. These diode lasers have the advantages that they may be modulated at gigahertz rates, and are available in an off-the-shelf

array format. The cathodes themselves may also be easily customized using bandgap engineering and lithography techniques developed for technologically mature III-V materials systems.

For many years, the importance of electron-electron interactions in moderate to high current probe forming systems has been known.^{12,13} These interactions produce three basic effects which are pertinent to system design. Stochastic interactions between electrons can cause broadening of the energy distribution of electrons in the beam; this phenomenon is known as the Boersch effect. Stochastic interactions also give rise to the trajectory displacement effect, which leads to a blurring of the final probe beam diameter at the image plane. The global space charge effect in the beam gives rise to defocusing and can generally be corrected for by controlling lens strength. Because the Boersch and trajectory displacement effects cannot be corrected for, they are of primary concern to us in this study. There has been a body of work on the simulation of these effects in electron beam instruments, including two programs commercially available for this purpose.^{14,15} We have developed a simulator which is optimized for the modeling of multiplexed primary and secondary sources, and for large numbers of electrons. In this article, we present an analysis of electron-electron interaction effects in a proposed NEA photocathode-based parallel electron beam direct write system.

II. THE PHYSICS OF NEGATIVE ELECTRON AFFINITY

The structure and principle of photoemission from an NEA photocathode is illustrated schematically in Figure 1. The photocathode consists of a semiconductor, usually a III-V compound such as GaAs, epitaxially grown on top of a diffusion blocking layer. This structure is bonded to a glass substrate, which has a anti-reflection coating on one side. The substrate provides the mechanical rigidity necessary to ensure the physical ruggedness of the overall cathode structure. The semiconductor layer itself is heavily p-doped ($1.5 \times 10^{19} \text{ cm}^{-3}$) so as to raise the conduction band relative to the Fermi level. The clean semiconductor surface is coated with a layer of Cs and O a few monolayers thick. The activation layer lowers the work function so that the conduction band in the bulk is above the vacuum level, a condition

of negative electron affinity. If electrons are excited into the conduction band within a diffusion length (typically a few microns) of the surface, many of them will diffuse to the surface where they will have a high probability of escaping into the vacuum.^{16,17} The electrons in a transmission mode photocathode may be excited using a red visible laser at approximately 635 nm, which is focused through the glass substrate onto the thin ($\sim 1 \mu\text{m}$) semiconductor bulk region. A diffraction-limited illuminating laser spot can be made as small as $0.5 \mu\text{m}$, and the emitted electrons will have a Gaussian spatial distribution of comparable dimensions. These emitted electrons may then be focused using electron optics on the opposite side of the photocathode surface.

III. SIMULATION OF COULOMB INTERACTIONS

A. ELECTRON OPTICAL TEST SYSTEM AND SPOT SIZE

Patterning 100 nm features in manufacturing requires the beam diameter to be no more than 30 - 40 nm to maintain linewidth control. The proposed design uses two lenses to demagnify an electron source of diameter of $0.5 \mu\text{m}$ by a factor of 15 (Figure 2). The minimum beam diameter as a function of the convergence angle at the image may be approximated by the quadrature sum of the beam diameters due to each component. The contributions of spherical aberration, chromatic aberration, diffraction, and demagnification to the minimum beam diameter are shown in Figure 3 for the values of C_s , C_c , and ΔV shown. It is clear from inspection of Figure 3 that the maximum attainable convergence angle at the wafer without significant spherical aberration is approximately 10 mrad corresponding to an acceptance angle at the source of 0.67 mrad. For a 50 kV beam and a uniformly distributed energy spread at the source of 0.2 eV, the total source divergence is 2 mrad. Taking into account the cosine distribution of the electrons at the source, this corresponds to a current efficiency of 36% (i.e. 36% of the emitted current reaches the target).

If the diameter of the source were reduced, less demagnification would be required for a given resolution and this would yield greater current efficiency. To this end, a similar system with $0.1\text{ }\mu\text{m}$ source diameter and lens focal lengths $f_1 = 60\text{ mm}$ and $f_2 = 15\text{ mm}$ was also simulated. These parameters lead to a demagnification of four with a convergence angle at the image of 8 mrad , which corresponds to a maximum convergence angle at the cathode of 2 mrad and a current efficiency approaching 100% for a $240\text{ }\mu\text{m}$ diameter aperture.

B. MONTE CARLO SIMULATION OF ELECTRON-ELECTRON INTERACTIONS

Electron-electron interactions may be simulated as a function of column parameters through a relatively straightforward Monte Carlo simulation process. As a significant amount of work on this subject has been performed and documented elsewhere, we shall describe only the essentials of the simulation below. The monograph by Jansen¹⁴ provides an excellent detailed description of this type of calculation. The overall strategy is first to set the initial conditions of electrons at the source using a random number generator to fit the angular and energy distributions of the emitted electrons to specified parameters. Each electron is emitted randomly within an interval of time determined by the source emission current. In each case, the energy distribution of the electrons is taken to be uniform. While this source model may not be wholly accurate, the descriptions of the velocity and angular distributions as a Gaussian and a cosine distribution are consistent with our earlier experimental observations for NEA photocathodes in sealed tubes.^{9,10} In fact, previous angular distribution measurements indicate that a slight forward focusing occurs for an NEA photocathode; thus, taking the distribution to be a cosine represents a conservative estimate.

After emission from the cathode, the electrons are accelerated through a 5 mm field region to 50 kV . There is a diverging lens action at the accelerating electrode which, if necessary, can be compensated by

a magnetic lens; this is neglected in our simulations. They are then focused through the objective lens, after which they may be intercepted by the aperture. Finally, the electrons are focused by the projector lens onto the wafer. The convergence angle is chosen so that lens aberrations are negligible. To isolate the effects due to electron-electron interactions, the aberration coefficients are set to zero. After the entire sample of electrons has been simulated, a data collection routine finds the plane of best focus by calculating the point at which the minimum $FW_{0.5}$ image blurring occurs.

To achieve acceptable statistics, the number of particles was chosen such that an increase in the sample size did not affect the calculated results for beam blurring and deflection. For example, where 10 nA beamlet currents were used, at least 200 particles per beamlet were simulated; the number of particles used for higher beamlet currents was proportional to the beamlet current as consistent with the above rule. For the most part, the beam statistics are quoted in terms of their $FW_{0.5}$ values, which refer to the widths of the distributions under which 50% of the particles fall. This statistic has been used widely in the literature because it is relatively insensitive to large deflections generated by very small numbers of events, such as the large deflections encountered in near misses between interacting electrons. In the parallel beam simulations, the statistics quoted are averages over the total number of beamlets.

C. RESULTS

For an array of 2×2 beams the final beam properties due to the beamlet current and the pitch (spacing) of beamlets at the source are shown in Figure 4. For beamlet currents of up to 50 nA, the beam blurring (FWHM) is relatively insensitive to pitch; as the beamlet current is further increased the blurring becomes significant. For a beamlet current of 200 nA, the blurring is 9 nm for a pitch of 10 μm , compared with 4 nm for a 200 μm pitch. A similar trend may be seen in the values for the $FW_{0.5}$ energy broadening (Boersch effect), shown in Figure 5.

To estimate how the previous results scale with higher total currents, a small individual beamlet current (10 nA) with correspondingly small blurring was taken as the base case, and the number of beams was

increased. Two configurations, one with a $0.5\ \mu\text{m}$ source diameter and one with a $0.1\ \mu\text{m}$ source diameter, were analyzed in terms of the blurring of the final image as a function of the total target current and the number of beams needed to achieve that current (Figure 6). With $0.5\ \mu\text{m}$ diameter sources, as can be obtained by focusing the incident laser light to a diffraction-limited spot, it appears that a beam current of $0.5\ \mu\text{A}$ can be obtained before beam blurring reaches $10\ \text{nm}$. This is achieved with an array of 144 (12×12) beamlets on a $50\ \mu\text{m}$ pitch. By using beamlet sources of $0.1\ \mu\text{m}$ diameter, we can achieve over $2.5\ \mu\text{A}$ before the blurring reaches $10\ \text{nm}$. Thus, there are significant advantages to using smaller sources, which may be achieved by restricting the emission area on the cathode surface.

Spurious deflection of a beamlet due to neighboring beamlets is obviously a concern. While the beam deflection does increase with current as a result of the global space charge effect, the worst-case deflection for 256 beams ($50\ \mu\text{m}$ pitch) at a total current of $2.5\ \mu\text{A}$ was $4\ \text{nm}$, less than half the beam blurring.

IV. DISCUSSION AND FUTURE WORK

Realizing a practical system is the obvious goal. To this end we have a number of tasks:

1. Continued modeling of different column configurations: This includes an analysis of the effects of the accelerating electrode, thick lenses, and off-axis aberrations. One advantage of this configuration is that we can trade off-axis aberrations for space charge effects by adjusting beamlet pitch. For the cases we have considered here the off-axis aberrations should not limit the field of view. For example, 16×16 sources on a $50\ \mu\text{m}$ pitch represent a field size of $800\ \mu\text{m}$ at the object and only $200\ \mu\text{m}$ at the wafer; Munro et al. indicated that immersion lenses (such as that used in the accelerating region) enjoy even lower aberrations than do conventional lenses¹⁸.

2. Experimental verification: Currently under construction in our laboratory is an ultrahigh vacuum (UHV) facility designed for the activation and testing of NEA photocathodes. The first part of the system consists of a chamber designed for cathode activations with Cs and O. This chamber may be used to test the spectral photoresponse of the cathodes, as well as to test novel activation procedures. The second portion of the facility is specially designed electron gun, in which various cathodes may be inserted, evaluated, and replaced under vacuum. This electron gun incorporates specialized electron optics designed to provide an optimal UHV environment for the cathode, since the cathode is sensitive to surface contamination. The third and final portion of the system is a versatile UHV electron optics column and chamber in which the emitted beam properties may be analyzed. Moreover, this chamber will serve as a test bed for the study of long-term stability and lifetime of the cathode source, during which time the effects of various materials typically found in semiconductor processing environments on cathode performance will be assessed. To date, both the activation and beam analysis chambers have been completed. A cathode has been successfully activated to a state of negative electron affinity with 22% quantum efficiency at 633 nm, and has been operated at 6 μ A for a period of time over ten hours with no indications of decay during preliminary stability and drift tests. The electron gun is currently being assembled, and will be tested soon after its completion.

3. Realization of 0.1 μ m source: With our existing cathode, the source diameter is minimized to 0.5 mm by focusing the laser illumination to a diffraction limited spot. Smaller sources will require a different approach, such as patterning the cathode to restrict the area of NEA to 0.1 μ m while retaining high brightness.

V. CONCLUSIONS

We have proposed a simple demagnifying system architecture for high-throughput electron beam lithography which relies on a high-performance negative electron affinity photocathode source.

Cathodes with different source diameters have been simulated, and resultant beam blurring and energy broadening for each system has been calculated for sources with different pitches and beamlet currents. The benefits of the high-brightness, low energy spread NEA source have been demonstrated with respect to both current efficiency and beam blurring. For the systems tested, electron-electron interactions do not appear to be limiting factor for a 0.1 μm system resolution and up to 2.5 mA at 50 kV.

ACKNOWLEDGMENTS

This work has been supported by the ARPA Advanced Lithography Program under ONR Grant #N0001492J1996. J. E. Schneider has been supported by an NSF Graduate Fellowship during the period of this work.

REFERENCES:

- ¹ S. D. Berger and J. M. Gibson, Appl. Phys. Lett. **57** (2), 153 (1990).
- ² G. Stengl *et al.*, J. Vac. Sci. Technol. B **9**, 2824 (1992).
- ³ M. B. Heritage, J. Vac. Sci. Technol. **12**, 1135 (1975).
- ⁴ J. Frosien, B. Lischke, and K. Anger, J. Vac. Sci. Technol. **16**, 1827 (1980).
- ⁵ W. H. Brunger, M. Torkler, and L. M. Buchman, J. Vac. Sci. Technol. B **10**, 2829 (1992).
- ⁶ T. H. Newman, R. F. W. Pease, and W. Devore, J. Vac. Sci. Technol. B **1**, 999 (1983).
- ⁷ Yasuda *et al.*, Jpn. J. Appl. Phys. **32** 6012 (1993).
- ⁸ C. N. Berglund, private communication.
- ⁹ A. W. Baum, W. E. Spicer, R. F. W. Pease, K. A. Costello, and V. W. Aebi, Proceedings of the 1995 SPIE International Symposium on Optical Science, Engineering, and Instrumentation **2522** 208.
- ¹⁰ A. W. Baum, W. E. Spicer, R. F. W. Pease, K. A. Costello, and V. W. Aebi, "Negative electron affinity photocathodes as high performance electron sources - Part 2: Energy spectrum measurements," *Proceedings of the 1995 SPIE International Symposium on Optical Science, Engineering, and Instrumentation*, **2550** 189.
- ¹¹ C. A. Sanford, Doctoral Thesis, Cornell University, 1990.
- ¹² A. N. Broers and H. C. Pfeiffer, Proceedings of the 11th Symposium on Electron, Ion and Laser Beam Technology, San Francisco, 1971 (unpublished).
- ¹³ H. C. Pfeiffer, Proceedings of the 5th Symposium on Scanning Electron Microscopy, Chicago, 1972 (unpublished), p. 113.
- ¹⁴ G. H. Jansen, *Coulomb Interactions in Particle Beams*, New York: Academic Press, 1990.
- ¹⁵ E. Munro, Nucl. Instrum. Methods Phys. Res. A **258**, 443 (1987).
- ¹⁶ W. E. Spicer, Phys. Rev. **112** (1958), 114.
- ¹⁷ C. N. Berglund and W. E. Spicer, Phys. Rev. **136** (1964) A1030 - A1044.
- ¹⁸ E. Munro, J. Orloff, R. Rutherford, and J. Wallmark, J. Vac. Sci. Technol. B **6**, 1971 (1988).

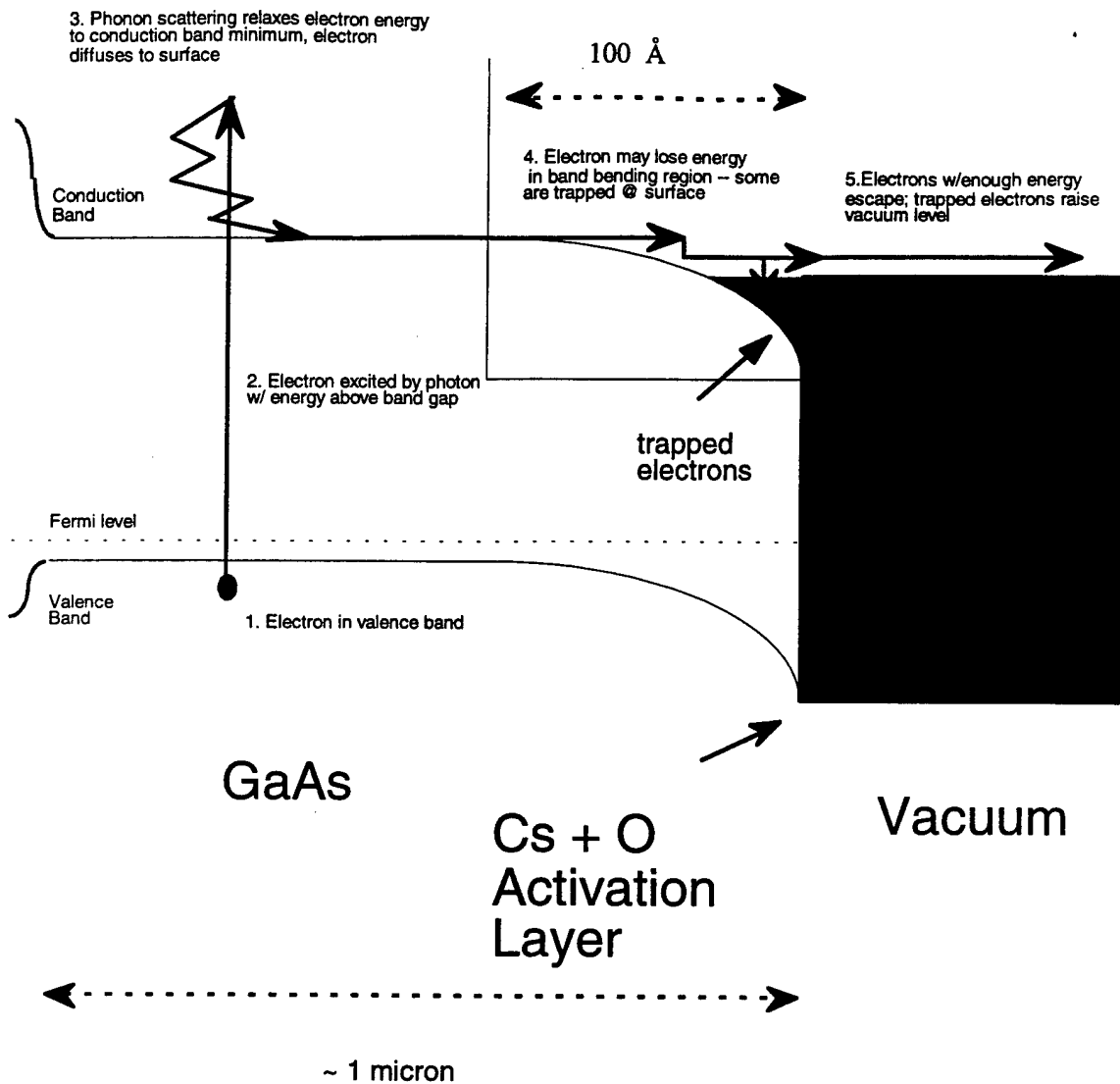


Figure 1: Band diagram of an NEA photocathode with a schematic of the photoemission process.

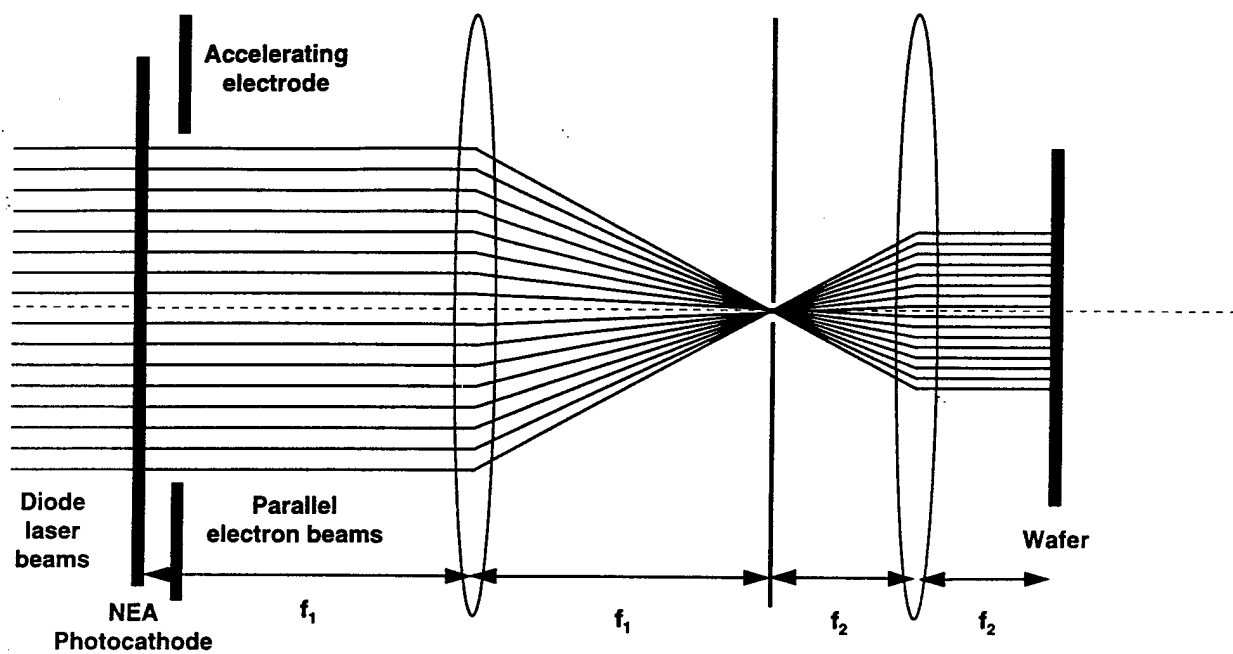


Figure 2: Simulated parallel electron beam lithography system configuration based on a negative electron affinity photocathode. Divergence due to the accelerating electrode can be compensated by an auxiliary magnetic lens and is absent. The lens are all represented as thin lenses.

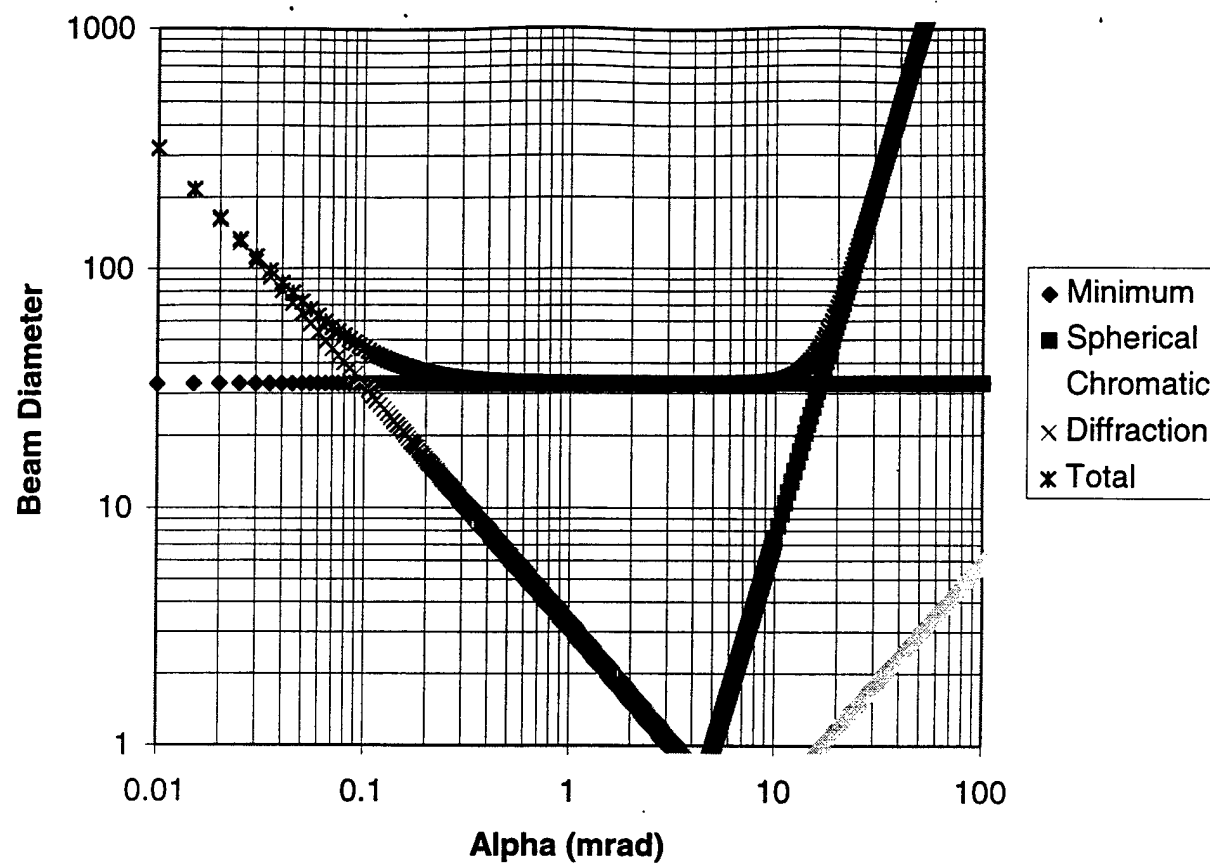


Figure 3: The effects of aberrations on beam diameter in the proposed system. The system parameters used are $f_2 = 15$ mm, $C_s = 18$ mm, $C_c = 15$ mm, $\Delta V = 0.2$ eV, and $V = 50$ kV.

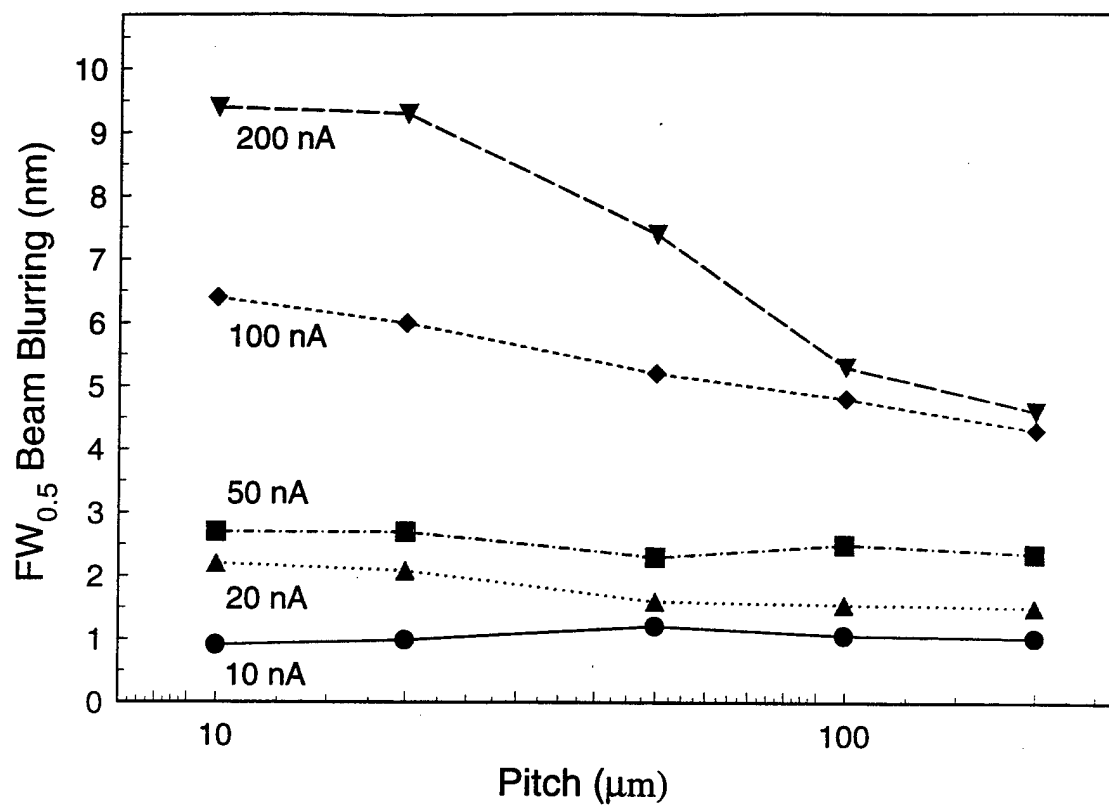


Figure 4: $FW_{0.5}$ beam blurring versus beamlet pitch for several beamlet currents. The data in each case represent the mean beam blurring in a four beam (2x2) system, with each beam carrying the indicated current.

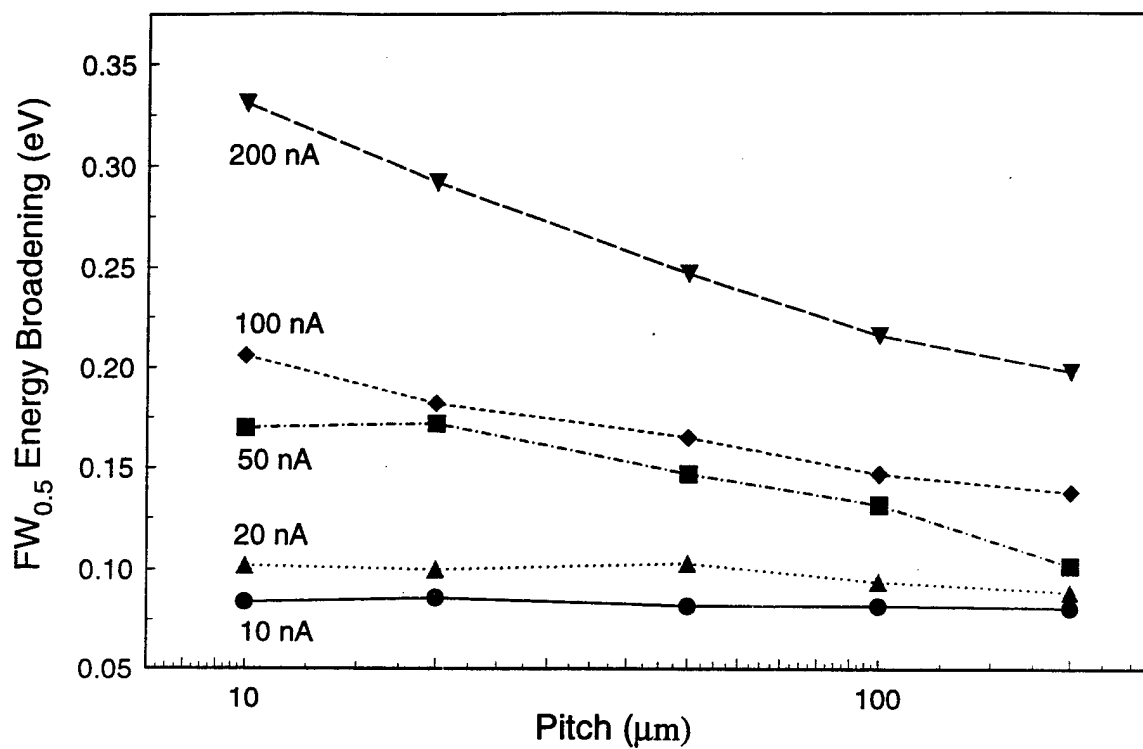


Figure 5: FW_{0.5} energy broadening versus beamlet pitch for several beamlet currents. The data in each case represent the mean beam blurring in a four beam (2x2) system, with each beam carrying the indicated current.

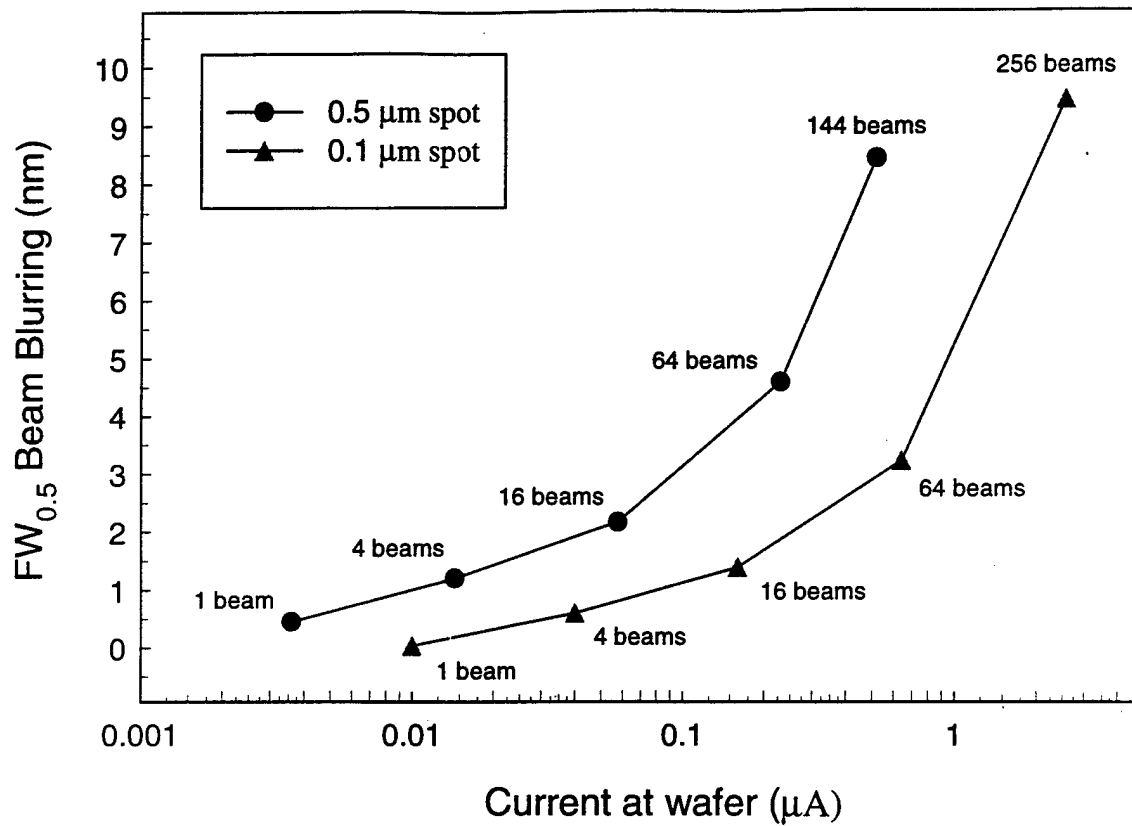


Figure 6: FW_{0.5} beam blurring versus the number of beams and total current at the wafer for both patterned and unpatterned cathodes. For a given system resolution, the patterned cathode requires less demagnification and requires approximately three times less current. Thus, for a given throughput, the use of a patterned cathode results in significantly less beam blurring.